BRIEF COMMUNICATION

LATERAL DIFFUSION IN BIOLOGICAL MEMBRANES

A NORMAL-MODE ANALYSIS OF DIFFUSION ON A SPHERICAL SURFACE

DENNIS E. KOPPEL, *Department of Biochemistry,* MICHAEL P. SHEETZ, *Department of Physiology,* AND MELVIN SCHINDLER, *Department of Microbiology, University of Connecticut Health Center, Farmington, Connecticut 06032 U.S.A.*

ABSTRACT A new approach is described for the analysis of lateral diffusion in biological membranes. It is shown that a suitably defined first moment of the concentration distribution on a spherical surface decays as a single exponential with a relaxation rate proportional to the diffusion coefficient and inversely proportional to the square of the radius of the sphere. The approach is illustrated with an example of fluorescence redistribution after photobleaching of membrane proteins in a spectrin-deficient spherocytic mouse erythrocyte membrane.

INTRODUCTION

In recent years, following the first demonstrations that integral membrane proteins can be free to diffuse in the plane of the membrane (1), considerable efforts have been made to allow the quantitative characterization of membrane translational dynamics. One general approach to the problem involves what is essentially a scaling-down of the classical free-diffusion-at-a-boundary experiment to the microscopic geometry of the cell surface. As an initial condition, an inhomogeneous concentration distribution of a particular component is induced within the cell membrane. Diffusion coefficients are calculated from the characteristic kinetics of the subsequent relaxation toward equilibrium. The initial inhomogeneity has been introduced by a variety of means: cell fusion (1–3), absorption bleaching (4, 5), spot-labeling (6), electrophoresis (7, 8), and fluorescence photobleaching (9–14). With a few exceptions (4, 5, 8) the redistribution toward equilibrium has been followed, in one way or another, by using fluorescent labels. Fluorescence photobleaching has been particularly popular as a concentration perturbation, because of the relative ease with which it can be routinely employed.

Recent major advances in technique (13, 14) have been directed toward the analysis of diffusion in an infinite plane, the geometry appropriate for monolayers of large adherent cells in culture or for reconstituted planar bilayers. The object of this paper is to present a new approach for the analysis of diffusion on a spherical surface, the geometry appropriate for

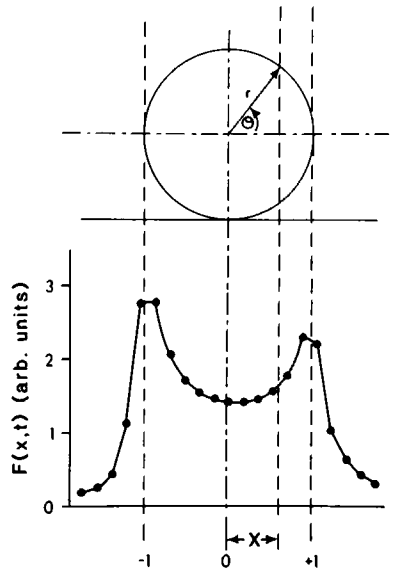

FIGURE 1 (Top) Schematic view of spherical cell of radius r as seen from the side, with polar axis parallel to the supporting planar substrate. The focused laser beam, incident from above, is scanned along the polar axis. (Bottom) Actual trace of fluorescence intensity as a function of $X = \cos \Theta$ monitored on a uniformly labeled (with DTAF) erythrocyte membrane with an incident laser wavelength of 4,765 Å. A ×100, 1.25 NA achromat focused the circularly symmetric laser beam onto the sample (minimum spot size <1.0 μm), and collected the fluorescence excited from the top and bottom surfaces of the cell.

cells in suspension or for large natural or reconstituted membrane vesicles. It is shown that, independent of the exact form of the initial concentration distribution, a suitably defined, measurable function of the distribution decays as a single exponential with a characteristic time inversely proportional to the diffusion coefficient.

THEORY

For an azimuthally symmetric concentration distribution characterized by a single lateral diffusion coefficient D on a spherical surface of radius r, the diffusion equation has the general solution (9, 15):

$$c(x, t) = \sum_{n=0}^{\infty} A_n P_n(x) \exp\left[-(1/2)n(n+1)\Gamma t\right], \tag{1}$$

where $\Gamma = 2D/r^2$ is the fundamental relaxation rate, x is the cosine of equatorial angle Θ (see Fig. 1), and $P_n(x)$ is the Legendre polynomial of order n. Coefficients A_n are determined by the particular initial concentration distribution, $c(x, 0)$.

In the normal-mode analysis introduced in this paper, it is not necessary to specify a particular functional form of $c(x, 0)$. We define a normalized "first moment" of the distribution:

$$\mu_1(t) = \int_{-1}^{1} P_1(x)c(x, t)\mathrm{d}x \Big/ \int_{-1}^{1} P_0(x)c(x, t)\mathrm{d}x, \tag{2}$$

where

$$P_0(x) = 1$$

$$P_1(x) = x.$$

Combining Eqs. 1 and 2, applying the orthogonality relation for the Legendre polynomials, it follows directly that $\mu_1(t)$ selects the first normal mode of the distribution, and that

$$\mu_1(t) = (A_1/3A_0) \exp(-\Gamma t). \tag{3}$$

Thus, if all labeled molecules had identical diffusion coefficients, $\mu_1(t)$ would decay as a single exponential. In general, for a mixed population of labeled components, $\mu_1(t)$ is a weighted sum or distribution of exponentials. A time-independent background component would be termed "immobile" on the time-scale of the experiment.

EXPERIMENTAL METHODS AND RESULTS

The general analytical approach described above can be illustrated with an example of a fluorescence redistribution after photobleaching (FRAP) experiment. In this case, values of $c(x, t)$ are estimated from experimental values of $F(x, t)$, the fluorescence intensity of an extrinsic fluorescent probe excited by a focused laser beam scanned along the polar axis of the sphere (see Fig. 1). The initial inhomogeneous concentration distribution is produced by a photobleaching pulse of intense laser light centered on the "edge" ($x = -1$) of the sphere. Photobleaching on the edge produces a nearly azimuthally symmetric concentration distribution as required, and acts to maximize the value of A_1 relative to the other coefficients of Eq. 1. Details of the experimental apparatus used to measure $F(x, t)$ and produce a photobleaching pulse have been presented elsewhere (14).

Fig. 2 presents a series of 1-s fluorescence scans recorded on a spectrin-deficient, spherocytic mouse erythrocyte membrane (16), with membrane proteins labeled with dichlorotriazinyl aminofluorescein (DTAF). The first scan was recorded before photobleaching. The others are the first few scans initiated consecutively at 2-s intervals after a 35-ms photobleaching pulse. Each scan shows the geometrical edge effect characteristic of a peripherally labeled spherical cell. Assuming a uniform prebleach concentration distribution, corrections for the effects of cell geometry and possible nonuniform illumination and

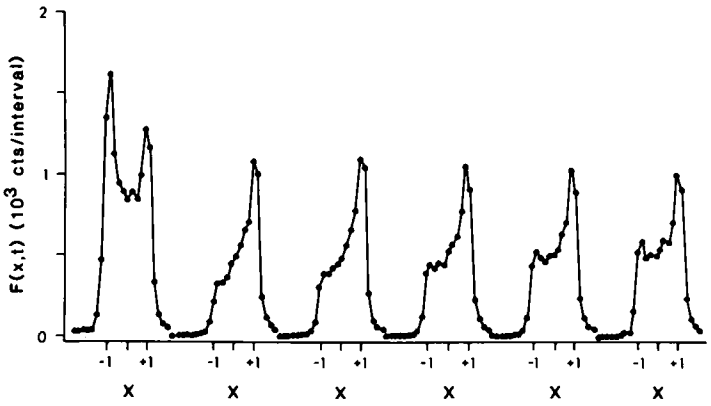

FIGURE 2 Series of 1-s fluorescence scans recorded on a DTAF labeled, spectrin-deficient, spherocytic mouse erythrocyte membrane with an incident laser power of 0.15 μW at 4,765 Å. The 2nd–6th scans were recorded at 2-s intervals after a 35-ms, 0.1 mJ bleaching laser-pulse centered on the leading ($x = -1$) edge of the cell.

collection efficiencies can be carried out to a good approximation in the calculation of $c(x, t)$ with point-by-point normalizations of each postbleach fluorescence scan by $F(x, -)$, a prebleach scan.

We can thus take

$$\hat{\mu}_1(t) = \hat{M}_1(t)/\hat{M}_0(t), \tag{4}$$

where

$$\hat{M}_1(t) = \frac{2}{N} \sum_{i=1}^{N} x_i F(x_i, t)/F(x_i, -)$$

$$\hat{M}_0(t) = \frac{2}{N} \sum_{i=1}^{N} F(x_i, t)/F(x_i, -),$$

as an experimental estimate of $\mu_1(t)$ (see Eq. 2). If there is reason to believe that the prebleach concentration distribution is significantly nonuniform (e.g., if a crosslinking ligand has introduced large-scale immobile patches or caps) one should consider normalizing $F(x_i, t)$ by an empirical estimate of the form of $F(x_i, -)$ expected for a uniform distribution.

Ideally, $M_0(t)$ is proportional to $\int_{-1}^{1} c(x, t)dx$, and is thus expected to be time-independent. In practice, the normalization by $\hat{M}_0(t)$ in the first moment defined above can serve to correct for possible slow experimental drifts (e.g., of laser intensity). It should also be noted at this time that because of the finite width of the monitoring laser beam, $\hat{\mu}_1(t)$, as defined above, is a biased estimate of $\mu_1(t)$; i.e., $\langle \hat{\mu}_1(t) \rangle$, the ensemble average of $\hat{\mu}_1(t)$ will necessarily deviate systematically from $\mu_1(t)$ to some extent. As discussed in the Appendix, however, there is every reason to believe that these deviations will not ordinarily be significant.

Fig. 3 presents semi-log plots for the data of Fig. 2. As a check of internal consistancy, $\hat{M}_0(t)$ and $\hat{M}_1(t)$ are plotted separately. For all practical purposes $\hat{M}_0(t)$ is time-independent. The relaxation of $\hat{M}_1(t)$ is seen to be monophasic and essentially complete (>90%) within experimental error. The solid straight lines are least-squares fits to the data, corresponding to a relaxation rate of 0.047 s^{-1}. For a cell radius of 2.25 μm, determined directly from a fluorescence scan, we can thus calculate a value of $D = 1.20 \times 10^{-9}$ cm^2/s. A more complete, controlled characterization and discussion of membrane protein diffusion in this cell system will appear elsewhere (17).

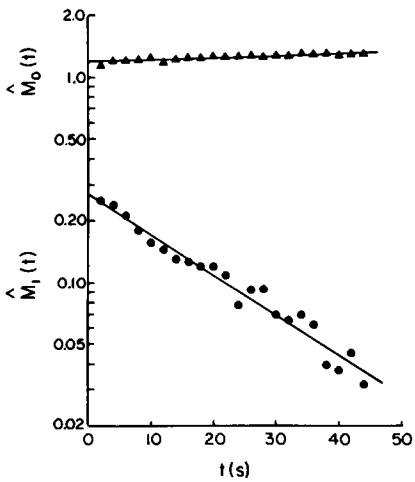

FIGURE 3 Semi-log plot of $\hat{M}_0(t)$ and $\hat{M}_1(t)$ as functions of time for the data of Fig. 2. Solid straight lines correspond to an estimated relaxation rate, Γ, of 0.047 s^{-1}.

DISCUSSION

The normal-mode analysis introduced above has two principal advantages over previous methods (8, 9, 12, 15, 18). It works for a large, general class of concentration distributions, requiring only an initial azimuthal symmetry. It is no longer necessary to produce a particular, prescribed initial distribution. The second advantage is that of analytical simplicity. It is relatively easy to analyse exponential decays, and detect deviations from a single exponential. An immobile component appears as a time-invariant background. In general, $\mu_1(t)$ is a sum or distribution of exponentials, making it possible to apply one of the several analytical procedures that have been developed to deal with this common situation (e.g., the method of cumulants; reference 19).

Primary emphasis has been placed on the characterization of the first normal mode, selected by the suitably defined first moment $\mu_1(t)$. For an initial condition symmetric about $x = 0$, however, analysis can proceed for an analogously defined second moment:

$$\mu_2(t) = \int_{-1}^{1} P_2(x)c(x, t)\mathrm{d}x \Big/ \int_{-1}^{1} P_0(x)c(x, t)\mathrm{d}x = (A_2/5A_0) \exp(-3\Gamma t) \tag{5}$$

(for a monodisperse recovery) where

$$P_2(x) = (1/2)(3x^2 - 1).$$

Under conditions in which D is small or r is large, $\mu_2(t)$ has the advantage of a characteristic time only ⅓ that of $\mu_1(t)$. A suitable initial condition for a second mode analysis could be provided in a FRAP experiment by two bleaching pulses, one centered at $x = -1$ and one centered at $x = +1$.

The normal-mode analysis introduced above has been applied successfully, in this paper and elsewhere (17), to fluorescence photobleaching experiments. Future applications should include the extension to other techniques, analyzing, for example, the intermixing of membrane components after cell fusion, or the back-diffusion of electrophoretically mobile receptors after electrophoresis.

APPENDIX

Effect of Finite Monitoring Beam Size

Experimental estimates of $c(x, t)$, determined from values of $F(x, t)/F(x, -)$, are actually spatial averages of $c(x, t)$ taken over finite ranges of x, weighted at each position by the product of the monitoring beam intensity and a geometrical weighting factor. This averaging procedure transforms each term in the series expansion of $c(x, t)$ (see Eq. 1) in a characteristic way, which can be represented in general as:

$$P_n(x) \rightarrow P_n(x) + f_n(x). \tag{A1}$$

The functions $f_n(x)$ are all either even (for even n) or odd (for odd n) functions about $x = 0$. This is a direct consequence of the symmetry of the cell geometry and the fact that the Legendre polynomials themselves are either even (for even n) or odd (for odd n) functions. It then follows that:

$$\langle \hat{M}_1(t) \rangle \alpha \frac{2}{3} A_1 \exp(-\Gamma t) + \sum_{\substack{n \\ \text{odd}}} A_n B_n \exp\left[-\left(\frac{1}{2}\right) n(n+1)\Gamma t\right], \tag{A2}$$

where

$$B_n = \int_{-1}^{1} x f_n(x) \mathrm{d}x.$$

Thus, the only correction terms of possible consequence appear for odd $n \geq 3$. These, however, can be expected to have sufficiently small amplitudes, and decay so rapidly relative to $e^{-\Gamma t}$, in any event, that they should not have a significant effect.

Similar correction terms (proportional to $\int_{-1}^{1} f_n(x)\mathrm{d}x$ for even n) can be written for $\langle \hat{M}_0(t) \rangle$, introducing a possible time dependence. The magnitude of this effect can be checked experimentally, and is shown in Fig. 3 to be insignificant.

This investigation was supported by research grants GM 23585 and HL 23795 from the U. S. Public Health Service. The authors would also like to thank Dr. Seldon Bernstein of the Jackson Memorial Laboratories at Bar Harbor, Maine, for supplying the spherocytic mice.

Received for publication 31 October 1979 and in revised form 20 December 1979.

REFERENCES

1. FRYE, L. D., and M. EDIDIN. 1970. The rapid intermixing of cell surface antigens after formation of mouse-human heterokaryons. *J. Cell Sci.* **7**:319–335.
2. FOWLER, V., and D. BRANTON. 1977. Lateral mobility of human erythrocyte integral membrane proteins. *Nature (Lond.)*. **268**:23–26.
3. SCHINDLER, M., D. E. KOPPEL, and M. P. SHEETZ. 1980. Modulation of membrane protein lateral mobility by polyphosphates and polyamines. *Proc. Natl. Acad. Sci. U.S.A.* In press.
4. POO, M.-M., and R. A. CONE. 1974. Lateral diffusion of rhodopsin in the photoreceptor membrane. *Nature (Lond.)*. **247**:438–441.
5. LIEBMAN, P. A., and G. ENTINE. 1974. Lateral diffusion of visual pigment in the photoreceptor disk membranes. *Science (Wash. D.C.)*. **185**:457–459.
6. EDIDIN, M., and D. FAMBROUGH. 1973. Fluidity of the cell surface of cultured muscle fibers. *J. Cell Biol.* **57**:27–53.
7. POO, M.-M., and K. R. ROBINSON. 1977. Electrophoresis of concanavalin A receptors along embryonic muscle cell membrane. *Nature (Lond.)*. **265**:602-605.
8. POO, M.-M., J. W. LAM, N. ORIDA, and A. W. CHAO. 1979. Electrophoresis and diffusion in the plane of the cell membrane. *Biophys. J.* **26**:1–22.
9. PETERS, R., J. PETERS, K. H. TEWS, and W. BAHR. 1974. A microfluorometric study of translational diffusion in erythrocyte membranes. *Biochim. Biophys. Acta.* **367**:282–294.
10. JACOBSON, K., E.-S. WU, and G. POSTE. 1976. Measurement of the translational mobility of concanavalin A in glycerol-saline solutions and on the cell surface by fluorescence recovery after photobleaching. *Biochim. Biophys. Acta.* **433**:215–222.
11. SCHLESSINGER, J., D. E. KOPPEL, D. AXELROD, K. JACOBSON, W. W. WEBB, and E. L. ELSON. 1976. Lateral transport on cell membranes: mobility of concanavalin A receptors on myoblasts. *Proc. Natl. Acad. Sci. U.S.A.* **73**:2409–2413.
12. EDIDIN, M., Y. ZAGYANSKY, and T. J. LARDNER. 1976. Measurements of membrane protein lateral diffusion in single cells. *Science (Wash. D.C.)*. **191**:466–468.
13. SMITH, B. A., and H. M. MCCONNELL. 1978. Determination of molecular motion in membranes using periodic pattern photobleaching. *Proc. Natl. Acad. Sci. U.S.A.* **75**:2759–2763.
14. KOPPEL, D. E. 1979. Fluorescence redistribution after photobleaching: a new multipoint analysis of membrane translational dynamics. *Biophys. J.* **28**:281–292.
15. HUANG, H. W. 1973. Mobility and diffusion in the plane of cell membrane. *J. Theor. Biol.* **40**:11–17.
16. GREENQUIST, A. C., S. B. SHOHET, and S. E. BERNSTEIN. 1978. Marked reduction of spectrin in hereditary spherocytosis in the common house mouse. *Blood.* **51**:1149–1155.
17. SHEETZ, M. P., M. SCHINDLER, and D. E. KOPPEL. 1980. The lateral mobility of integral membrane proteins is increased in spectrin-deficient spherocytic erythrocytes. *Nature (Lond.)*. In press.
18. LARDNER, T. J., and N. SOLOMON. 1976. The determination of local cell membrane diffusion coefficients. *J. Theor. Biol.* **60**:433–440.
19. KOPPEL, D. E. 1972. Analysis of macromolecular polydispersity in intensity correlation spectroscopy: the method of cumulants. *J. Chem. Phys.* **57**:4814–4820.